applied sciences

Article

Degradation-Aware Monitoring of Vanadium Redox Flow Batteries Using Multi-Model Adaptive Estimation

Shazeb H. Syed [1], Ammar E. Ali [2] and Sohel Anwar [3,*]

[1] Mechanical Engineering, Purdue University, West Lafayette, IN 47907, USA; syed62@purdue.edu
[2] Electrical Engineering Technology, Purdue University, West Lafayette, IN 47907, USA; ali67@purdue.edu
[3] Mechanical Engineering, Purdue University, Indianapolis, IN 46202, USA
* Correspondence: sanwar@purdue.edu

Abstract

Reliable condition monitoring of vanadium redox flow batteries (VRFBs) is essential for ensuring safe and efficient operation under varying stress conditions. This study presents a model-based operating-condition classification framework based on Multi-Model Adaptive Estimation (MMAE) for real-time identification of battery operating regimes. A reduced-order equivalent circuit model is used to represent battery dynamics, and condition-specific parameter sets are obtained offline using Particle Swarm Optimization (PSO) methodology to build a model bank. Four operating conditions derived from Accelerated Stressor Lifetime Testing (ASLT) datasets are considered: nominal operation (1.6 V, cycle 5), high-voltage operation (1.8 V, cycle 5), aged operation (1.6 V, cycle 70), and combined aged and high-voltage operation (1.8 V, cycle 70). For each of these operating conditions, an extended Kalman filter (EKF)-based residual generation scheme is developed and embedded within the MMAE framework to evaluate model likelihoods and update operating-condition probabilities in real time. The proposed MMAE-based approach was able to successfully identify the specific operating regimes and detect the transitions between stress conditions using only terminal current and voltage measurements. This study demonstrates that distinct operating conditions produce identifiable voltage signatures, enabling accurate and computationally efficient classification. The proposed methodology thus offers a robust framework for degradation-aware monitoring of VRFB systems, which could be leveraged in a battery management system for improved battery life.

Keywords: vanadium redox flow battery; condition monitoring; particle swarm optimization; extended Kalman filter; multi-model adaptive estimation; equivalent circuit model; degradation detection; parameter identification

Check for updates

Academic Editor: Paolo Di Leo

Received: 13 May 2026
Revised: 26 June 2026
Accepted: 2 July 2026
Published: 15 July 2026

1. Introduction

The increasing penetration of renewable energy sources such as wind and solar has intensified the need for long-duration reliable energy storage systems capable of mitigating intermittency and ensuring grid stability [1,2]. Among the available technologies, vanadium redox flow batteries (VRFBs) have emerged as a promising solution due to their intrinsic safety, long cycle life, and unique ability to decouple power and energy capacity through independent scaling of the stack and electrolyte volumes [3,4]. These characteristics make VRFBs particularly suitable for grid-scale applications, renewable energy integration, and mission-critical infrastructure.

VRFB operation is governed by redox reactions involving vanadium ions in multiple oxidation states, enabling stable cycling without cross-contamination effects [3]. However, despite their advantages, VRFBs are subject to performance degradation over extended cycling, particularly under high-voltage operating conditions. Degradation mechanisms such as electrolyte imbalance, membrane aging, and loss of electrochemical activity significantly influence the behavior of the system and the characteristics of the terminal voltage [1,4]. Accelerated stressor lifetime testing (ASLT) studies have demonstrated that elevated upper cutoff voltages (1.7–1.8 V) accelerate degradation and lead to irreversible efficiency losses [5,6], highlighting the need for robust condition-monitoring strategies.

To model VRFB behavior, both physics-based electrochemical models and reduced-order equivalent circuit models (ECMs) have been developed. Electrochemical models provide detailed insight into transport phenomena and reaction kinetics but are computationally expensive and unsuitable for real-time applications [7–9]. In contrast, ECMs offer a simplified representation using lumped resistive and capacitive elements to capture ohmic, activation, and concentration overpotentials [10,11]. Enhanced ECM formulations, such as those proposed by Xiong et al. [12] and Zhang et al. [13], have demonstrated improved accuracy in reproducing VRFB voltage dynamics across varying operating conditions.

The effectiveness of ECM-based approaches depends strongly on accurate parameter identification. Traditional estimation techniques such as recursive least squares (RLS) are sensitive to noise and may yield unstable or nonphysical parameter values under nonlinear conditions [14]. Evolutionary optimization methods, particularly Particle Swarm Optimization (PSO), have shown superior performance in handling nonlinear, multimodal optimization problems without requiring gradient information [15,16]. PSO has been successfully applied to battery modeling, demonstrating improved convergence stability and voltage reconstruction accuracy compared to conventional methods [12,17,18].

While significant progress has been made in VRFB modeling and parameter estimation, most existing approaches rely on a single model representation and do not explicitly account for multiple operating regimes. In practical applications, VRFBs operate under varying conditions such as nominal operation, high-voltage stress, aging, and combined degradation scenarios. These conditions lead to distinct parameter variations and voltage signatures that cannot be effectively captured using a single adaptive model.

Multi-Model Adaptive Estimation (MMAE) provides a probabilistic framework for addressing this limitation by maintaining a bank of candidate models and updating their likelihoods based on measurement residuals [19,20]. This approach has been previously applied in lithium-ion battery diagnostics and fault detection, enabling robust classification of operating conditions using limited measurements. However, its application to VRFB systems remains limited, particularly in conjunction with experimentally derived degradation datasets.

In this context, the present work integrates PSO-based parameter identification with an MMAE-based monitoring framework for VRFBs. Experimentally validated ASLT datasets are used to construct condition-specific ECM parameter sets representing nominal, high-voltage, aged, and combined operating states. These models are embedded within an EKF–MMAE architecture to enable real-time probabilistic classification using only terminal voltage and current measurements. This approach bridges the gap between accurate parameter identification and robust multi-condition classification, providing a computationally efficient and experimentally grounded solution for VRFB condition monitoring. This work uniquely combines global optimization-based parameter identification with probabilistic multi-model classification using experimentally validated degradation datasets.

The main contributions of this work are summarized as follows:

- Development of a reduced-order equivalent circuit model-based condition monitoring framework for VRFBs.
- Application of Particle Swarm Optimization for robust parameter identification under multiple degradation regimes.
- Integration of Extended Kalman Filter observers with a Multi-Model Adaptive Estimation framework for probabilistic operating condition classification.
- Experimental validation using accelerated stressor lifetime testing datasets representing nominal, high-voltage, aged, and combined stress conditions.

2. Materials and Methods

This study presents a model-based degradation-aware condition monitoring framework for vanadium redox flow batteries (VRFBs), integrating reduced-order equivalent circuit modeling, Particle Swarm Optimization (PSO) for parameter identification, Extended Kalman Filtering (EKF) for state estimation, and Multi-Model Adaptive Estimation (MMAE) for probabilistic classification of operating regimes. The overall workflow consists of (i) experimental data acquisition, (ii) model development, (iii) parameter identification, and (iv) multi-model classification.

The overall workflow of the proposed condition-monitoring framework is illustrated in Figure 1.

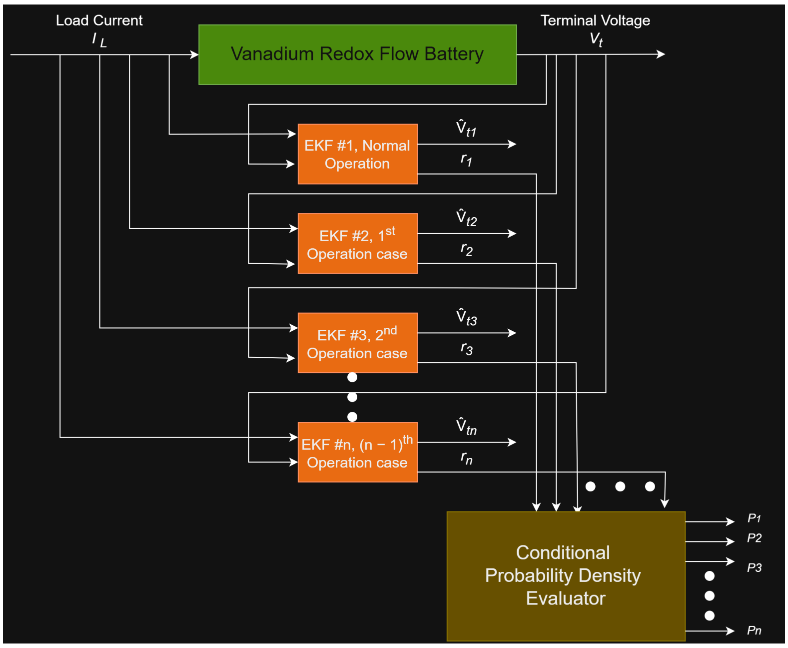

Figure 1. Overall workflow of the proposed VRFB condition-monitoring framework. Accelerated stressor lifetime testing datasets are used for particle swarm optimization-based equivalent circuit parameter identification to generate condition-specific models. Extended Kalman Filter (EKF) observers estimate internal states and generate voltage residuals for each candidate model, and the Multi-Model Adaptive Estimation framework updates model probabilities to classify the operating regime in real time.

2.1. Experimental Dataset and Preprocessing

The experimental dataset used in this study is derived from Accelerated Stressor Lifetime Testing (ASLT) experiments conducted on a single-cell VRFB [9]. These experiments subject the battery to controlled cycling under varying voltage limits to emulate degradation behavior. The operating voltage range is 0.8–1.8 V, with a nominal voltage of approximately 1.25 V, and the system is operated at a constant current density under controlled temperature and flow conditions. The ASLT datasets used in this study were adopted from the experimental reliability investigation reported by Patel et al. [5].

Four operating conditions derived from Accelerated Stressor Lifetime Testing (ASLT) datasets are considered:

- Nominal operation: 1.6 V, cycle 5;
- High-voltage operation: 1.8 V, cycle 5;
- Aged operation: 1.6 V, cycle 70;
- Combined aged and high-voltage operation: 1.8 V, cycle 70.

The operating conditions correspond to experimentally derived degradation regimes obtained from Accelerated Stressor Lifetime Testing datasets. Elevated upper cutoff voltages accelerate polarization growth, electrolyte imbalance, membrane stress, and vanadium crossover mechanisms, while repeated cycling contributes to long-term aging effects, altered electrochemical kinetics, electrode surface deposition, and changes in electrode porosity and active surface area. These degradation mechanisms influence internal resistance and polarization behavior, resulting in distinct voltage-response characteristics under each operating condition. Consequently, the operating conditions represent physically meaningful degradation scenarios associated with distinct electrochemical behavior rather than purely statistical labels.

Representative voltage profiles from the ASLT study are shown in Figure 2.

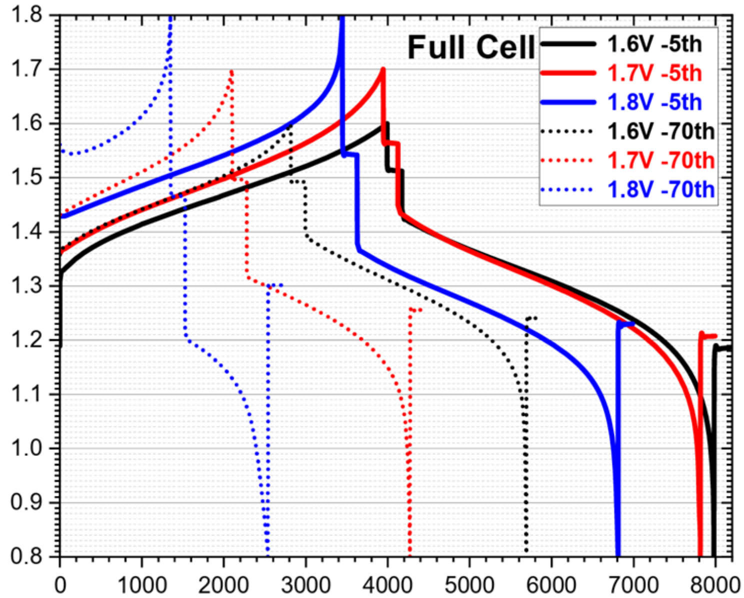

Figure 2. Voltage profiles obtained from accelerated stressor lifetime testing experiments for cutoff voltages of 1.6 V, 1.7 V, and 1.8 V at Cycle 5 and Cycle 70. The divergence between early-cycle and aged-cycle responses illustrates degradation-induced changes in voltage behavior under elevated voltage stress [5].

The dataset consists of time-series measurements of terminal voltage and current. Raw data are preprocessed by removing noise artifacts, aligning time indices, and resampling signals to ensure uniform discretization. The datasets are divided into identification and validation segments, where the former is used for parameter estimation and the latter for classification evaluation.

The voltage and current measurements were uniformly resampled using a sampling interval of 1 s prior to implementation of the discrete-time EKF framework. Uniform discretization was selected to ensure numerical stability and consistent recursive observer updates across all operating conditions.

The experimental conditions corresponding to the ASLT dataset are summarized in Table 1.

Table 1. Specifications of the ASLT experimental setup.

Configuration	Value
Voltage Range	0.8–1.8 V
Current Density	80 mA cm^{-2}
Number of Cells	1
Cell Area	49 cm^2
Vanadium Concentration	1.6 mol/L
Nominal Voltage	1.25 V
Coulombic Efficiency	93–94%
Temperature	25 °C
Flow Rate	80 mL min^{-1}

2.2. Equivalent Circuit Model Development

To enable real-time monitoring, a reduced-order equivalent circuit model (ECM) is adopted to represent VRFB dynamics. The model consists of an ohmic resistance and two resistor–capacitor (RC) networks representing activation and concentration overpotentials. This structure captures dominant voltage dynamics while maintaining computational efficiency.

The reduced-order equivalent circuit structure adopted in this work is shown in Figure 3.

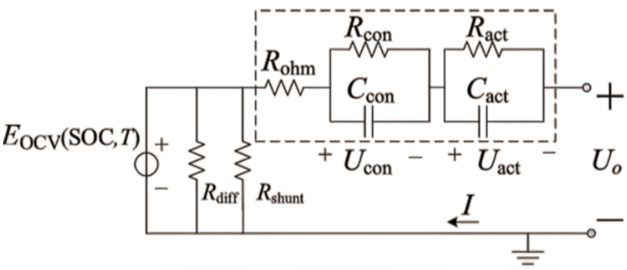

Figure 3. Five-element equivalent circuit model used to represent the dynamic voltage behavior of the vanadium redox flow battery. The model consists of an ohmic resistance representing electrolyte and contact losses, together with two resistor–capacitor polarization branches representing activation and concentration overpotentials.

The terminal voltage is expressed as:

$$V_t = E_{OCV}(SOC) - IR_{ohm} - V_{act} - V_{con} \tag{1}$$

The polarization dynamics are modeled as:

$$\dot{V}_{act} = -\frac{1}{R_{act}C_{act}}V_{act} + \frac{1}{C_{act}}I \tag{2}$$

$$\dot{V}_{con} = -\frac{1}{R_{con}C_{con}}V_{con} + \frac{1}{C_{con}}I \tag{3}$$

The state vector consists of state of charge (SOC) and polarization voltages, while the parameter vector includes:

$$\theta = [R_{ohm}, R_{act}, C_{act}, R_{con}, C_{con}]$$

2.3. Parameter Identification Using Particle Swarm Optimization

Accurate parameter identification is critical for ECM performance. In this work, PSO is employed to identify optimal model parameters for each operating condition. Unlike traditional recursive least squares methods, PSO provides a global optimization framework capable of handling nonlinear and multimodal search spaces.

The PSO-based parameter identification procedure used in this study is summarized in Figure 4.

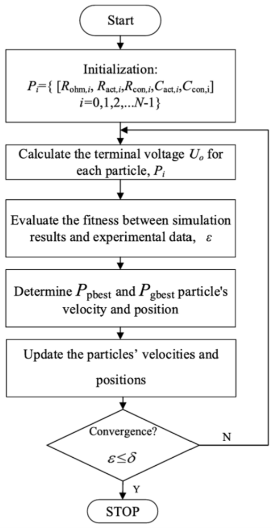

Figure 4. Flowchart of the particle swarm optimization algorithm used for equivalent circuit model parameter identification. Each particle represents a candidate parameter set, and the optimization iteratively updates particle positions until the voltage reconstruction error converges.

The objective function minimized during optimization is defined as:

$$J(\theta) = \sum_{k=1}^{N} (V_{meas}(k) - V_{model}(k, \theta))^2 \quad (4)$$

where V_{meas} and V_{model} represent measured and predicted terminal voltages, respectively.

The optimization is performed within physically constrained bounds to ensure realistic parameter values. The PSO algorithm iteratively updates particle positions based on inertia, cognitive, and social components until convergence is achieved. This process is repeated independently for each operating regime, resulting in condition-specific parameter sets that form a fixed model bank. The PSO parameters, including swarm size, inertia weight, and learning coefficients, were selected empirically to ensure stable convergence.

2.4. State Estimation Using Extended Kalman Filter

For each model in the parameter bank, an Extended Kalman Filter is implemented to estimate internal states in real time. The nonlinear discrete-time system is represented as:

$$x_{k+1} = f(x_k, u_k) + w_k \quad (5)$$

$$y_k = h(x_k, u_k) + v_k \quad (6)$$

where x_k is the state vector, u_k is the input current, and y_k is the measured terminal voltage. The process noise w_k and measurement noise v_k are assumed to be Gaussian.

The EKF performs recursive prediction and update steps, linearizing the nonlinear model at each time step. This enables estimation of SOC and polarization voltages while generating residual signals for each candidate model.

The EKF operates in parallel for each model in the bank, generating residual signals used for probabilistic classification in the MMAE framework. The process and measurement noise covariance matrices were tuned empirically to balance estimation accuracy and robustness against measurement noise.

The process-noise and measurement-noise covariance matrices were empirically tuned to balance observer convergence speed and robustness against measurement disturbances. Stable probability convergence and residual behavior were observed across all evaluated operating conditions using the selected covariance settings. Since the present work represents an exploratory study focused on degradation-aware operating-condition classification, detailed robustness analysis under varying covariance settings and adaptive noise estimation methods were not investigated and will be considered in future work.

Additionally, the EKF formulation adopted in this work assumes Gaussian process and measurement noise for recursive state estimation. Thus, robustness against explicitly non-Gaussian noise distributions and severe nonlinear sensor disturbances was not investigated in the present study.

2.5. Multi-Model Adaptive Estimation Framework

The Multiple Model Adaptive Estimation (MMAE) framework is employed to classify the operating condition of the VRFB under multiple degradation regimes. In this framework, multiple candidate models operate simultaneously while receiving the same measured current input. Each candidate model is associated with an Extended Kalman Filter (EKF) observer that generates predicted terminal voltage responses corresponding to a specific operating condition.

Unlike conventional single-model estimation approaches, MMAE evaluates multiple candidate operating regimes in parallel and determines the most probable operating condition based on observer residual behavior. Since each candidate model represents a distinct experimentally derived operating condition, the framework can explicitly distinguish among nominal, high-voltage, aged, and combined degradation scenarios.

For the i-th candidate model, the voltage residual is defined as:

$$r_i(k) = V_{\text{meas}}(k) - V_{i,\text{pred}}(k) \tag{7}$$

where $V_{\text{meas}}(k)$ is the measured terminal voltage, and $V_{i,\text{pred}}(k)$ is the observer-predicted terminal voltage corresponding to model i.

This residual serves as the statistical input to the MMAE likelihood calculation. When the predicted output of a candidate model closely matches the measured battery response, the associated residual approaches zero, indicating a higher likelihood that the operating condition corresponds to that model.

The innovation variance associated with the i-th model is expressed as:

$$S_i(k) = C_i P_i^-(k) C_i^T + R_i \tag{8}$$

where C_i is the output Jacobian matrix, $P_i^-(k)$ is the predicted EKF covariance matrix before correction, and R_i is the measurement-noise covariance associated with model i.

Assuming Gaussian measurement noise, the likelihood of model i explaining the measured voltage response at time step k is computed as:

$$L_i(k) = \exp\left(-\frac{1}{2}\frac{r_i^2(k)}{S_i(k)}\right) \tag{9}$$

A higher likelihood corresponds to a smaller voltage residual, indicating stronger agreement between the measured and predicted voltage responses.

The model probabilities are recursively updated using Bayesian normalization:

$$p_i(k) = \frac{L_i(k)p_i(k-1)}{\sum_{j=1}^{M} L_j(k)p_j(k-1)} \tag{10}$$

where

- $p_i(k)$ is the posterior probability assigned to model i at time step k;
- $p_i(k-1)$ is the prior probability from the previous sampling instant;
- M is the total number of candidate models in the condition-specific model bank.

The normalization process ensures that the total probability remains equal to unity:

$$\sum_{i=1}^{M} p_i(k) = 1 \tag{11}$$

The active operating regime is identified as the model corresponding to the highest posterior probability:

$$m^*(k) = \arg\max_i p_i(k) \tag{12}$$

This probabilistic framework enables explicit classification of VRFB operating conditions rather than implicit parameter tracking. Since each candidate model represents a distinct experimentally derived degradation scenario, the MMAE framework can discriminate among nominal, high-voltage, aged, and combined degradation regimes in real time.

Furthermore, the recursive probability-update mechanism improves robustness against transient operating variations and measurement uncertainty. By continuously evaluating voltage residuals and updating model probabilities, the framework enables smooth transitions between operating-condition estimates during concatenated dataset evaluation.

2.6. Model Implementation and Validation

The proposed EKF–MMAE framework operates at each sampling instant using measured terminal current and voltage inputs obtained from Accelerated Stressor Lifetime Testing (ASLT) datasets. The ASLT datasets used in this study were adopted from the experimental reliability investigations reported by Patel et al. [5], where VRFB degradation behavior under elevated upper cutoff voltages was experimentally characterized.

The ASLT methodology accelerates degradation by subjecting the VRFB to controlled cycling under elevated charging voltages and repeated operating cycles. These accelerated stress conditions enable efficient generation of degradation datasets representative of long-term VRFB aging behavior while significantly reducing experimental testing duration.

Four operating conditions derived from the ASLT datasets are considered in this work:

- Nominal operation: 1.6 V, cycle 5;
- High-voltage operation: 1.8 V, cycle 5;
- Aged operation: 1.6 V, cycle 70;
- Combined aged and high-voltage operation: 1.8 V, cycle 70.

For each operating condition, a condition-specific equivalent circuit model is generated using the offline PSO-based parameter-identification framework developed in the authors' previous work [18]. These experimentally derived parameter sets are subsequently used to construct the condition-specific model bank employed within the MMAE framework.

During online implementation, all EKF observers operate simultaneously while receiving the same measured current input. Each observer independently generates internal-state estimates and predicted terminal voltage responses corresponding to its associated operating condition. The resulting voltage residuals are processed through the Bayesian probability-update equations to determine the most probable operating regime in real time.

The validation procedure was conducted using concatenated ASLT datasets containing sequential transitions among nominal, high-voltage, aged, and combined degradation conditions. This concatenated evaluation structure enables assessment of the framework under dynamic operating-regime transitions rather than isolated steady-state operating conditions.

Model performance is evaluated using voltage reconstruction accuracy, residual behavior, convergence of model probabilities, and operating-condition classification capability. The probability trajectories generated by the MMAE framework provide direct insight into classification confidence and model discrimination performance during operating-condition transitions.

Since the computationally intensive parameter-identification procedure is performed offline, the online implementation only requires EKF state estimation and probabilistic model evaluation. This significantly reduces computational burden and makes the proposed framework computationally efficient for real-time battery-management applications.

The online implementation consists of four low-order EKF observers operating in parallel with Bayesian probability updates. Since the computationally intensive PSO optimization procedure is performed offline, the online implementation requires only low-dimensional matrix operations suitable for embedded battery-management applications. The average execution time for one complete operating cycle was approximately 1.18 s (1180 ms) using MATLAB (R2026a) implementation on a standard desktop computing platform. Since the reported execution time corresponds to an entire operating cycle rather than individual sampling steps, the effective computational burden per EKF update remains low. Evaluation on embedded hardware platforms such as ARM Cortex-M systems was not investigated in the present study and will be considered in future work.

The overall implementation establishes a transition from offline parameter identification toward real-time degradation-aware monitoring and probabilistic operating-condition classification for VRFB systems. By integrating experimentally derived degradation models with observer-based probabilistic classification, the proposed framework provides a physically interpretable and experimentally validated approach for VRFB condition monitoring.

3. Results

3.1. Parameter Identification Performance

Condition-specific parameter sets were identified for each operating condition to construct the fixed model bank used in the MMAE framework. Compared to recursive least squares (RLS), PSO demonstrated significantly improved voltage reconstruction accuracy. The voltage reconstruction performance is evaluated using root mean square error (RMSE). The identified models demonstrate accurate voltage reconstruction, indicating that the model bank provides a reliable foundation for MMAE-based classification.

Figure 5 illustrates the comparison between experimental voltage and model predictions obtained using PSO and RLS. The PSO-based model accurately tracks both transient and steady-state behavior, whereas RLS exhibits noticeable deviations, particularly during dynamic transitions.

The Recursive Least Squares implementation utilized a forgetting factor of $\lambda = 0.995$ to balance parameter adaptation and noise suppression. The initial covariance matrix was selected as $P_0 = 10^3 I$ to provide sufficient parameter sensitivity during early iterations while maintaining numerical stability during recursive estimation. Both PSO and RLS utilized identical ECM structures and experimental datasets to ensure fair comparison.

A quantitative comparison between PSO- and RLS-based parameter identification is presented in Table 2.

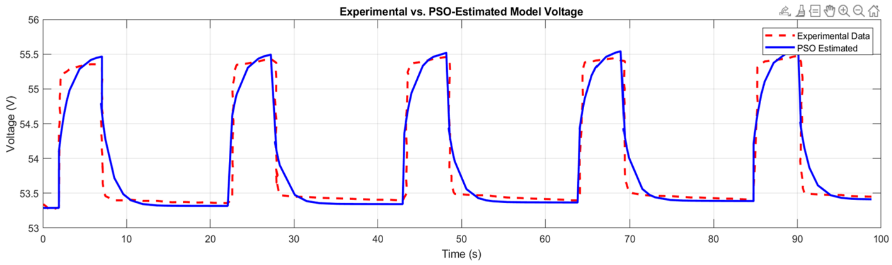

(a) Terminal voltage reconstruction using particle swarm optimization identified equivalent circuit parameters

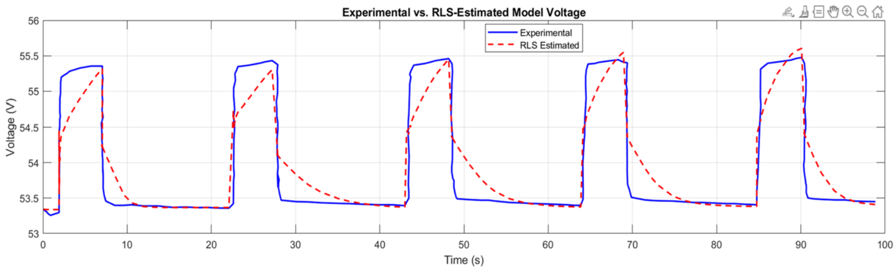

(b) Terminal voltage reconstruction using recursive least squares estimation identified equivalent circuit parameters

Figure 5. Comparison of terminal voltage reconstruction using (**a**) particle swarm optimization-identified equivalent circuit parameters and (**b**) recursive least squares estimation. The PSO-based model more accurately captures transient and steady-state voltage behavior under pulse-current excitation [18].

Table 2. Comparison of PSO and RLS parameter estimation performance [18].

Parameter	PSO	RLS
R_{ohm}	0.03 Ω	0.071 Ω
R_{act}	0.03 Ω	0.025 Ω
C_{act}	43.55 F	3999.3 F
R_{con}	0.0208 Ω	0.001 Ω
C_{con}	5624.53 F	10000 F
RMSE	0.037 V	0.233 V

The PSO-based parameter identification presented in this work was performed using a single experimental dataset for each operating condition. The reported RMSE values were computed by comparing the identified model responses against experimentally measured reference voltage data. Since repeated stochastic optimization trials were not conducted in the present study, statistical metrics such as standard deviation and confidence intervals were not evaluated.

3.2. PSO Convergence and Parameter Evolution

The convergence behavior of the particle swarm optimization algorithm is analyzed by examining the evolution of the identified equivalent circuit model parameters over iterations. Figure 6 shows the trajectories of the ohmic resistance and polarization parameters for the nominal dataset (Data001).

The smooth convergence of parameters indicates stable optimization behavior and confirms the suitability of PSO for nonlinear ECM identification. The convergence behavior confirms that the PSO algorithm identifies physically consistent parameter values across iterations. The convergence behavior indicates that the PSO algorithm effectively balances global exploration and local exploitation, ensuring stable identification of physically meaningful parameters.

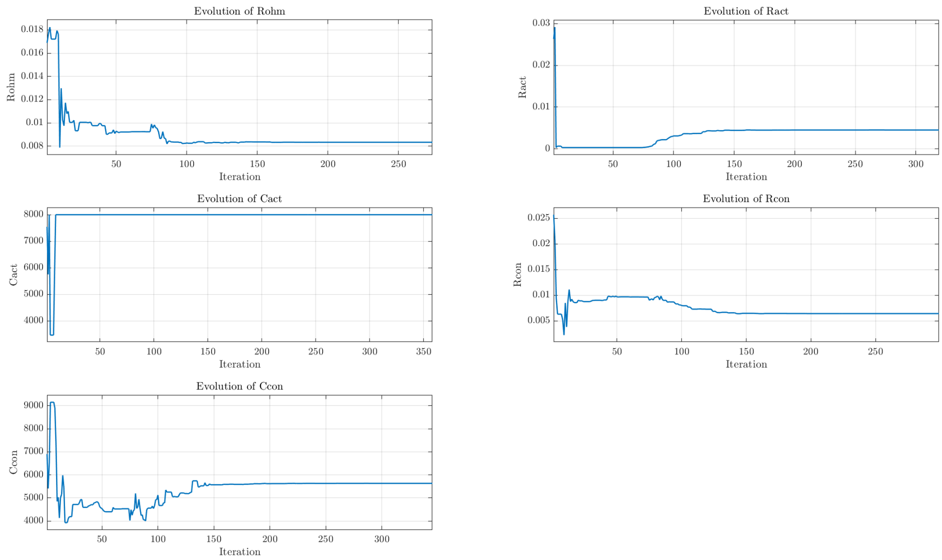

Figure 6. Evolution of equivalent circuit model parameters during particle swarm optimization for the nominal dataset (Data001). The parameter trajectories converge toward stable values, demonstrating effective optimization convergence.

All parameters converge toward stable values within a finite number of iterations, indicating effective exploration and convergence of the optimization process. Initial fluctuations are observed due to stochastic particle movement; however, the algorithm rapidly stabilizes as particles converge toward the global optimum.

This convergence behavior confirms the robustness of PSO in identifying physically consistent parameter sets for nonlinear battery models.

3.3. Model Validation and Identified Parameter Analysis

The identified ECM parameters were validated under nominal operating conditions. The voltage reconstruction performance under nominal operating conditions is presented in Figure 7.

The parameter bounds summarized in Table 3 define the feasible search space used during the PSO-based equivalent circuit parameter-identification process. These limits were selected through iterative preliminary tuning to ensure physically meaningful parameter values while maintaining stable optimization convergence across all operating conditions.

The lower and upper resistance bounds were selected to capture realistic variations in ohmic, activation, and concentration losses observed in VRFB systems under different degradation regimes. In particular, wider limits were assigned to the concentration resistance term to account for degradation-induced mass-transport limitations and electrolyte imbalance under aged and high-voltage operating conditions.

Table 3. Final parameter bounds used in PSO-based ECM identification after tuning for stable convergence and physically consistent parameter estimation.

Parameter	Lower Bound	Upper Bound
R_{ohm}	0.001 Ω	0.05 Ω
R_{act}	0.001 Ω	0.05 Ω
C_{act}	10 F	10,000 F
R_{con}	0.001 Ω	0.5 Ω
C_{con}	10 F	20,000 F

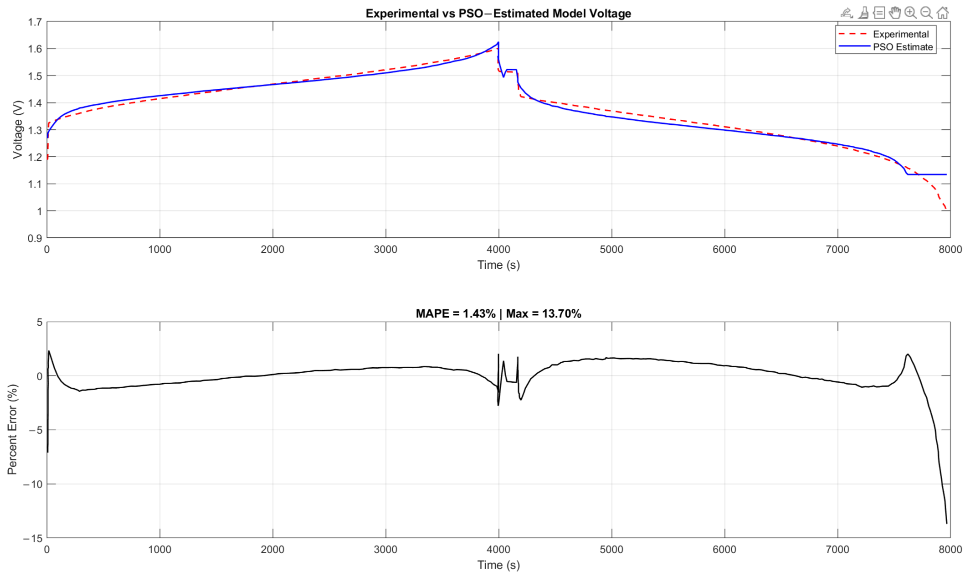

Figure 7. Experimental and PSO-estimated terminal voltage for the nominal operating condition. The reduced-order equivalent circuit model accurately reproduces the charge, peak, and discharge regions, with a mean absolute percentage error of 0.94%.

Similarly, the capacitance bounds were selected to capture both fast and slow transient polarization dynamics associated with electrochemical charge-transfer processes and ion diffusion behavior. Larger upper limits for the capacitance parameters enable the ECM to represent long-duration transient voltage responses observed during charging and discharging cycles.

These parameter bounds provide sufficient flexibility for the optimization process while preventing convergence toward nonphysical solutions. Consequently, the selected search-space limits improve optimization robustness and ensure consistent parameter identification across multiple degradation conditions.

The final parameter sets identified using PSO for each operating condition are summarized in Table 4. These parameters correspond to the four operating regimes derived from the ASLT datasets and represent the identified system characteristics under different stress conditions.

Table 4. PSO-identified ECM parameters for different operating conditions.

Parameter	Nominal	High-V	Aged	Combined
R_{ohm} (Ω)	0.0084	0.0019	0.0035	0.016
R_{act} (Ω)	0.004	0.003	0.003	0.026
C_{act} (F)	8000	3101.57	4001.43	395.75
R_{con} (Ω)	0.0064	0.034	0.033	0.215
C_{con} (F)	5631.98	8000	10000	12000

Parameter sensitivity was evaluated by comparing incrementally stressed operating conditions corresponding to 1.6 V, 1.7 V, and 1.8 V cycling conditions (Table 5). The identified ECM parameters exhibited systematic variation with increasing voltage stress, particularly in the polarization-related resistance and capacitance terms. Variations in C_{act}, R_{con}, and C_{con} indicate sensitivity of transient electrochemical dynamics to degradation-induced changes under elevated voltage-stress conditions. These parameter trends support practical parameter identifiability within the selected operating conditions.

Table 5. Incremental variation of identified ECM parameters under increasing voltage-stress conditions.

Parameter	$\Delta(1.6\ V \rightarrow 1.7\ V)$	$\Delta(1.7\ V \rightarrow 1.8\ V)$
R_{ohm} (Ω)	+0.0002	−0.0067
R_{act} (Ω)	+0.0127	−0.0137
C_{act} (F)	−6539	+1641
R_{con} (Ω)	−0.0054	+0.0330
C_{con} (F)	+6368	−4000

The PSO-identified ECM parameters presented in Table 4 demonstrate clear variations across the nominal, high-voltage, aged, and combined degradation operating conditions. These parameter variations reflect degradation-induced changes in internal electrochemical behavior and transport dynamics within the VRFB system.

The nominal operating condition exhibits relatively low ohmic and concentration resistance values, indicating reduced internal losses and stable electrochemical performance. Under the high-voltage operating condition, increases in concentration resistance suggest the onset of enhanced polarization and electrolyte transport limitations caused by elevated charging voltages.

The aged operating condition demonstrates further parameter variation associated with long-term cycling degradation. In particular, changes in activation and concentration parameters indicate altered electrochemical kinetics and increased mass-transport losses resulting from degradation of internal cell components and electrolyte imbalance.

The combined aged and high-voltage condition exhibits the largest overall resistance values, indicating the cumulative effect of voltage-induced stress and long-term cycling degradation. This operating condition produces the most severe polarization behavior and the largest deviation from nominal voltage-response characteristics.

Overall, the parameter variations observed across the four operating conditions generate distinct voltage-response signatures that improve the discriminative capability of the MMAE framework during operating-condition classification. These results demonstrate that the identified ECM parameters effectively capture degradation-related changes in VRFB dynamic behavior.

3.4. Operating Regime Classification

The Multiple Model Adaptive Estimation (MMAE) framework is used to classify the operating regime of the vanadium redox flow battery using a bank of condition-specific equivalent circuit models. Each model corresponds to one of the four operating conditions: nominal, high-voltage, aged, and combined stress. The transition delay observed during regime switching is minimal, indicating rapid adaptation of the probabilistic framework.

Figure 8 demonstrates the classification of a single operating regime (high-voltage) with MMAE correctly identifying the operating condition.

Figure 9 presents the classification results for a concatenated dataset consisting of sequential transitions between different operating regimes. The top subplot shows the measured and simulated terminal voltage, demonstrating accurate voltage tracking across all regimes. The middle subplot illustrates the evolution of model probabilities, while the bottom subplot shows the selected active model based on the highest probability. The classification is performed using the parameter sets summarized in Table 4, where each model represents a distinct operating regime.

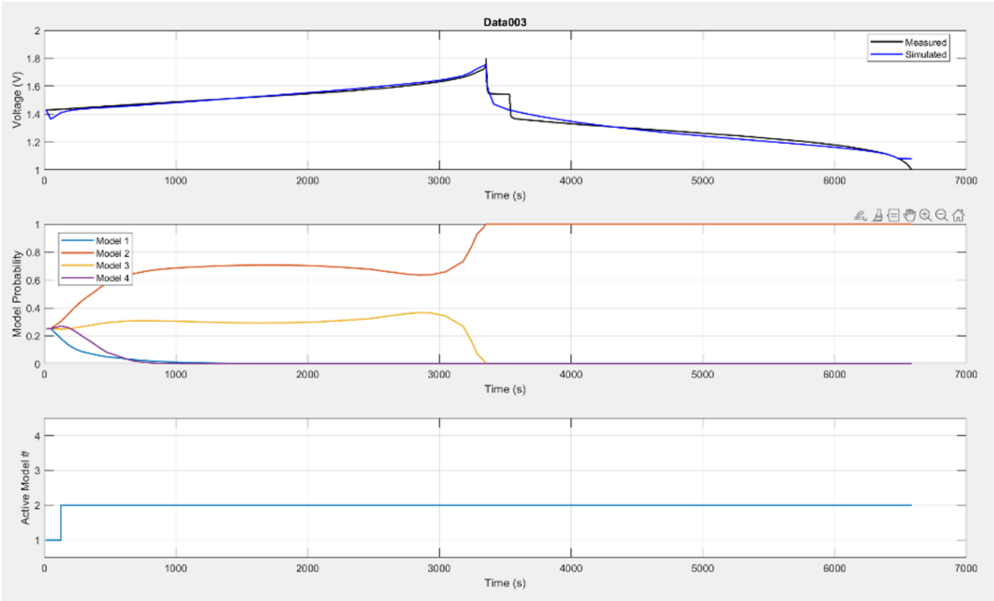

Figure 8. MMAE-based operating-condition classification results for the high-voltage operating condition dataset (1.8 V, cycle 5). The top subplot compares measured and observer-estimated terminal voltages, the middle subplot presents the evolution of model probabilities, and the bottom subplot shows the active model selected by the MMAE framework over time.

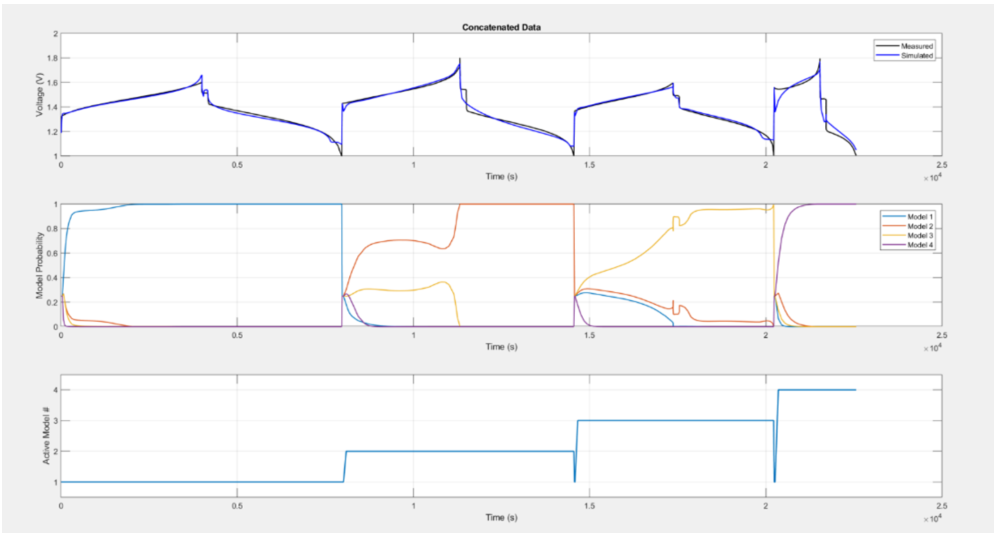

Figure 9. Measured and simulated terminal voltage, model probability evolution, and active model selection for the concatenated accelerated stressor lifetime testing dataset. The Multiple Model Adaptive Estimation framework successfully identifies transitions among nominal, high-voltage, aged, and combined operating regimes.

The model probabilities converge rapidly toward the correct operating regime under stationary conditions, indicating strong discrimination capability. During transitions between regimes, temporary overlap in model probabilities is observed; however, the transition delay is minimal, indicating rapid adaptation of the probabilistic classification framework. This demonstrates the ability of the MMAE approach to detect changes in battery operating conditions in real time.

The EKF observers continuously estimate SOC-dependent voltage dynamics and internal polarization behavior during charging and discharging operation. Consequently, the generated residuals reflect both transient SOC variation and operating-condition-dependent parameter mismatch. Transient probability overlap observed during operating-condition transitions is partially attributable to SOC-related transient behavior. However, the recursive Bayesian probability-update mechanism mitigates transient misclassification by evaluating likelihood evolution over time rather than relying solely on instantaneous residual magnitude.

The MMAE probability trajectories demonstrated stable convergence toward the correct operating condition during both isolated and concatenated dataset evaluations. Transition regions exhibited temporary probability overlap caused by transient voltage dynamics; however, the correct operating regime remained dominant after convergence. The classification framework maintained consistent operating-condition discrimination capability throughout sequential operating-regime transitions.

The reduced-order ECM captures dominant VRFB voltage dynamics, including ohmic, activation, and concentration polarization behavior. Gas evolution, vanadium crossover, membrane-side reactions, and electrolyte side reactions are not explicitly modeled within the present framework. These degradation effects are indirectly reflected through experimentally identified parameter variations obtained under degraded operating conditions. Consequently, the ECM represents aggregate degradation-induced voltage behavior rather than detailed electrochemical side-reaction dynamics.

The present framework focuses on classification among experimentally derived operating regimes obtained from ASLT datasets. Intermediate degradation states or previously unseen operating conditions may produce probability overlap among candidate models due to partial similarity in voltage-response behavior. The evaluation of intermediate degradation conditions such as cycle 30 or 1.7 V operating conditions was outside the scope of the present study.

The results confirm that distinct operating regimes produce identifiable voltage signatures due to variations in internal resistance and polarization dynamics. By leveraging these differences, the proposed framework provides explicit classification of battery conditions rather than relying on implicit parameter adaptation.

Overall, the MMAE-based classification approach enables robust and interpretable condition monitoring using only terminal voltage and current measurements, making it suitable for real-time battery management applications. The classification accuracy is validated through correct regime selection across all segments of the concatenated dataset.

4. Discussion

The results demonstrate that the integration of global optimization, state estimation, and probabilistic classification provides a robust framework for VRFB condition monitoring.

The superior performance of PSO over RLS highlights the importance of global optimization in nonlinear parameter identification. RLS methods are sensitive to noise and may converge to suboptimal solutions, whereas PSO effectively explores the parameter space and identifies physically meaningful values. This improvement is reflected in the significant reduction in voltage reconstruction error.

The reduced-order equivalent circuit model provides a balance between computational efficiency and physical interpretability. While high-fidelity electrochemical models offer deeper insight, their complexity limits real-time applicability. The ECM used in this study captures dominant dynamics with minimal computational burden, making it suitable for online monitoring.

The EKF enables reliable estimation of internal states using only terminal measurements. This is particularly important for practical battery management systems where internal states are not directly measurable. The residuals generated by the EKF form the foundation for probabilistic classification.

The experimental datasets include charging and discharging regions containing transient voltage behavior near elevated SOC conditions and steep voltage-transition regions. Although the reduced-order ECM captures dominant voltage dynamics, increased residual magnitudes were observed near highly nonlinear operating regions due to stronger electrochemical nonlinearity and polarization effects. The EKF observers maintained stable state-estimation behavior under these operating conditions.

The MMAE framework provides a key advantage over traditional single-model approaches by explicitly distinguishing between operating regimes. Instead of continuously adapting parameters, the proposed method identifies discrete conditions such as aging and high-voltage stress. This improves interpretability and enables more actionable diagnostics.

Furthermore, the use of experimentally derived ASLT datasets ensures that the framework is validated under realistic degradation scenarios. The ability to detect transitions between regimes demonstrates the robustness of the approach under dynamic conditions.

Overall, the results confirm that combining PSO, EKF, and MMAE provides a scalable and computationally efficient solution for degradation-aware monitoring of VRFB systems. Unlike conventional single-model approaches, the proposed framework explicitly distinguishes between multiple degradation regimes using a model bank derived from experimentally validated datasets, enhancing interpretability and diagnostic capability. A limitation of the proposed framework is the reliance on a fixed model bank constructed from predefined operating conditions. In practical applications, unseen degradation modes may require adaptive updating of the model bank. A limitation of the proposed framework is the reliance on a fixed model bank derived from predefined operating conditions. In practical applications, unseen degradation modes may require adaptive updating of the model bank.

5. Conclusions

This study presents a model-based condition monitoring framework for vanadium redox flow batteries, integrating reduced-order equivalent circuit modeling, Particle Swarm Optimization for parameter identification, Extended Kalman Filtering for state estimation, and Multi-Model Adaptive Estimation for probabilistic classification.

Experimental datasets obtained from Accelerated Stressor Lifetime Testing were used to characterize four operating regimes: nominal, high-voltage, aged, and combined stress conditions. PSO-based parameter identification significantly improved voltage reconstruction accuracy compared to recursive least squares, reducing RMSE from 0.233 V to 0.037 V.

The Extended Kalman Filter enabled reliable estimation of internal states and generation of residual signals using only terminal current and voltage measurements. The proposed MMAE framework successfully classified the operating regimes differentiating between normal and degraded battery states and detected transitions between those conditions in real time.

The key contribution of this work lies in the application of a Multi-Model Adaptive Estimation (MMAE) methodology for explicit operating-condition classification in vanadium redox flow batteries. By leveraging a model bank derived from experimentally validated datasets, the proposed framework enables reliable identification of nominal, high-voltage, aged, and combined operating conditions using only terminal voltage and current measurements.

The results demonstrate that MMAE provides a robust and computationally efficient approach for detecting degradation-related operating regimes and transitions in real time. This establishes MMAE as a powerful framework for degradation-aware monitoring of VRFB systems, offering improved interpretability compared to conventional single-model approaches.

Future work will focus on the investigation of statistical repeatability across multiple optimization runs as well as the evaluation of EKF under non-Gaussian measurement conditions and adaptive filtering approaches. In addition, implementation of the proposed algorithm on embedded hardware platforms such as ARM Cortex-M systems will be considered as future work.

Author Contributions: Conceptualization, S.A.; methodology, S.A.; software, S.H.S. and A.E.A.; validation, S.A., S.H.S. and A.E.A.; resources, S.A.; data curation, S.H.S. and A.E.A.; writing—original draft preparation, S.H.S.; writing—review and editing, S.H.S., A.E.A. and S.A.; visualization, S.H.S.; supervision, S.A.; project administration, S.A.; funding acquisition, S.A. All authors have read and agreed to the published version of the manuscript.

Funding: This research received no external funding.

Institutional Review Board Statement: Not applicable.

Informed Consent Statement: Not applicable.

Data Availability Statement: The original contributions presented in the study are included in the article, further inquiries can be directed to the corresponding author.

Conflicts of Interest: The authors declare no conflict of interest.

Abbreviations

The following abbreviations are used in this manuscript:

VRFB	Vanadium Redox Flow Battery
ECM	Equivalent Circuit Model
PSO	Particle Swarm Optimization
EKF	Extended Kalman Filter
MMAE	Multiple Model Adaptive Estimation
ASLT	Accelerated Stressor Lifetime Testing
RLS	Recursive Least Squares
SOC	State of Charge
OCV	Open-Circuit Voltage
RMSE	Root Mean Square Error
MAPE	Mean Absolute Percentage Error
RC	Resistor–Capacitor

References

1. Wang, Y.; Mu, A.; Wang, W.; Yang, B.; Wang, J. A review of capacity decay studies of all-vanadium redox flow batteries: Mechanism and state estimation. *ChemSusChem* **2024**, *17*, e202301787. [CrossRef] [PubMed]
2. Ulaganathan, M.; Aravindan, V.; Yan, Q.; Madhavi, S.; Skyllas-Kazacos, M.; Lim, T.M. Recent advancements in all-vanadium redox flow batteries. *Adv. Mater. Interfaces* **2016**, *3*, 1500309.
3. Skyllas-Kazacos, M.; Cao, L.; Kazacos, M.; Kausar, N.; Mousa, A. Vanadium electrolyte studies for the vanadium redox battery—A review. *ChemSusChem* **2016**, *9*, 1521–1543. [CrossRef] [PubMed]
4. Yuan, X.Z.; Song, C.; Platt, A.; Zhao, N.; Wang, H.; Li, H.; Fatih, K.; Jang, D. A review of all-vanadium redox flow battery durability: Degradation mechanisms and mitigation strategies. *Int. J. Energy Res.* **2019**, *43*, 6599–6638.
5. Patel, R.; Huang, Q.; Li, B.; Crawford, A.; Sivakumar, B.M.; Song, C.; Jiang, Z.; Platt, A.; Fatih, K.; Reed, D. Reliability studies of vanadium redox flow batteries: Upper limit voltage effect. *RSC Adv.* **2024**, *14*, 34381–34389. [CrossRef] [PubMed]
6. Huang, Q.; Crawford, A.; Song, C.; Jiang, Z.; Platt, A.; Fatih, K.; Bock, C.; Jang, D.; Reed, D. *Reliability Investigation of All-Vanadium Redox Flow Batteries*; Technical Report; Pacific Northwest National Laboratory and National Research Council Canada: Ottawa, ON, Canada, 2023.
7. Puleston, T.; Clemente, A.; Costa-Castelló, R.; Serra, M. Modelling and estimation of vanadium redox flow batteries: A review. *Batteries* **2022**, *8*, 121. [CrossRef]

8. Weber, A.Z.; Mench, M.M.; Meyers, J.P.; Ross, P.N.; Gostick, J.T.; Liu, Q. Redox flow batteries: A review. *J. Appl. Electrochem.* **2011**, *41*, 1137–1164. [CrossRef]
9. Li, Z.; Wang, F.; Huang, Z. Numerical analysis and research on mass transfer performance of vanadium redox flow battery. *J. Electrochem. Soc.* **2024**, *171*, 060519. [CrossRef]
10. Mohamed, M.R.; Ahmad, H.; Abu Seman, M.N. Estimating the state-of-charge of all-vanadium redox flow battery. *Elektron. Elektrotechnika* **2013**, *19*, 37–42. [CrossRef]
11. Das, J.; Dasgupta, R. A review and analysis of electrical equivalent circuit models of vanadium redox flow battery. In *Emerging Electronics and Automation*; Springer: Berlin/Heidelberg, Germany, 2022; pp. 183–192.
12. Xiong, R.; Yang, Y.; Tang, J.; Li, Y.; Wei, Z.; Su, Y.; Zhang, Q. An enhanced equivalent circuit model of vanadium redox flow battery energy storage systems considering thermal effects. *IEEE Access* **2019**, *7*, 162297–162308. [CrossRef]
13. Zhang, Y.; Zhao, J.; Wang, P.; Skyllas-Kazacos, M.; Xiong, B.; Badrinarayanan, R. A comprehensive equivalent circuit model of all-vanadium redox flow battery for power system analysis. *J. Power Sources* **2015**, *290*, 14–24. [CrossRef]
14. Jarraya, I.; Degaa, L.; Rizoug, N.; Chabchoub, M.H.; Trabelsi, H. Comparison study between hybrid PSO and RLS for battery parameter estimation. *J. Energy Storage* **2022**, *50*, 104424.
15. Shi, Y.; Eberhart, R. A modified particle swarm optimizer. In Proceedings of the 1998 IEEE International Conference on Evolutionary Computation Proceedings, Anchorage, AK, USA, 4–9 May 1998.
16. Coello, C.A.C.; Pulido, G.T.; Lechuga, M.S. Handling multiple objectives with particle swarm optimization. *IEEE Trans. Evol. Comput.* **2004**, *8*, 256–279. [CrossRef]
17. Mesbahi, T.; Khenfri, F.; Rizoug, N.; Chaaban, K.; Bartholomeus, P.; Le Moigne, P. Dynamical modeling of Li-ion batteries. *Electr. Power Syst. Res.* **2016**, *131*, 195–204. [CrossRef]
18. Syed, S.H.; Ali, A.; Anwar, S. Parameter identification of ECM model of a vanadium redox flow battery using particle swarm optimization. In Proceedings of the ASME International Mechanical Engineering Congress and Exposition, Memphis, TN, USA, 16–20 November 2025; pp. 1–7.
19. Singh, A.; Izadian, A.; Anwar, S. Model-based condition monitoring in lithium-ion batteries. *J. Power Sources* **2014**, *268*, 459–468. [CrossRef]
20. Rahman, M.A.; Anwar, S.; Izadian, A. Electrochemical model-based condition monitoring via experimentally identified Li-ion battery model and HPPC. *Energies* **2017**, *10*, 1266. [CrossRef]

https://doi.org/10.3390/app16147079